Post-synthetic Covalent Grafting of Amines to NH_2-MOF for Post-Combustion Carbon Capture

*Anita Justin,[a] Jordi Espín,[a] Miriam Jasmin Pougin,[b] Dragos Stoian,[c] Till Schertenleib,[a] Mounir Mensi,[d] Ilia Kochetygov,[a,e] Andres Ortega-Guerrero[b] and Wendy L. Queen[a]**

Anita Justin, Jordi Espín, Till Schertenleib, Ilia Kochetygov, Wendy L. Queen

[a] École Polytechnique Fédérale de Lausanne (EPFL), Institute of Chemical Sciences and Engineering (ISIC), Laboratory for Functional Inorganic Materials (LFIM), CH-1951 Valais, Switzerland.

Email: wendy.queen@epfl.ch

Miriam Jasmin Pougin, Andres Ortega-Guerrero

[b] École Polytechnique Fédérale de Lausanne (EPFL), Institute of Chemical Sciences and Engineering (ISIC), Laboratory of Molecular Simulation (LSMO), CH-1951 Valais, Switzerland.

Dragos Stoian

[c] Swiss-Norwegian Beamlines (SNBL), European Synchrotron Radiation Facility (ESRF), 38000 Grenoble, France.

Mounir Mensi

[d] École Polytechnique Fédérale de Lausanne (EPFL), CH-1951 Valais, Switzerland.

Ilia Kochetygov

[e] Paul Scherrer Institut (PSI), CH-5232 Villigen, Switzerland.

Metal-Organic Frameworks, Post-synthetic modification, Covalent amine grafting, Carbon dioxide capture.

ABSTRACT: Herein, we report a post-synthetic modification strategy to covalently graft polyamines, including ethylenediamine (ED), diethylenetriamine (DETA), tris(2-aminoethyl)amine (TAEA), and polyethyleneimine (PEI) to the amino-ligand of a Cr-MOF, NH_2-Cr-BDC, for post-combustion carbon capture applications. X-ray absorption spectroscopy (XAS) and X-ray photoelectron spectroscopy (XPS) reveal that ~45% of the MOF ligands are grafted with polyamines. Also, after assessment of CO_2 uptake,

CO_2/N_2 selectivity, isosteric heats of CO_2 adsorption, separation performance during humid CO_2/N_2 (15/85) breakthrough experiments, and cyclability, the study reveals an enhanced performance for the polyamine composites and the following performance trend: NH_2-Cr-BDC<ED<DETA<TAEA<PEI. The best-performing materials, including TAEA and PEI-grafted MOFs, offer CO_2 uptakes of 1.0 and 1.55 mmol/g, respectively, at 0.15 bar and 313 K. Further, these composites also offer a high CO_2 capacity after 200 temperature swing adsorption/desorption (TSA) cycles in simulated humid flue gas. Last, after soaking the composites in water, we show that there is no loss of CO_2 capacity; on the contrary, when the same MOF is impregnated with polyamines using traditional approaches, there is ~85 % CO_2 capacity loss after soaking. Thus, this covalent grafting strategy successfully immobilizes amines in MOF pores preventing leaching and hence could be an effective strategy to extend adsorbent lifetime.

1. Introduction

Climate change, which is an undeniable concern that poses a major risk to humanity and ecological systems alike, stems from greenhouse gas (GHG) emissions that originate from an assortment of anthropogenic activities, like electricity production.[1-2] Of the GHGs that are emitted into the air, it is estimated that CO_2 alone accounts for ~76%, making carbon capture from large point sources an urgent need.[3] To date, the most mature capture technology consists of aqueous liquid amine scrubbers.[4] While these solutions can readily extract large amounts of CO_2 from gas mixtures, liquid amines are also corrosive, suffer from high regeneration energies, and often degrade over time.[4-5] These shortfalls, combined with the high heat capacity of these liquids,[6] leads to a large energy penalty with their implementation.[4] In fact, it was estimated that the implementation of liquid amine capture could decrease the efficiency of a power plant by as much as 30%.[4] Given this, increasing numbers of studies are aimed at designing CO_2 selective solid adsorbents, an effort which might cut the parasitic energy cost by as much as 50%.[5]

Of the many possible classes of solid, porous materials to choose from for CO_2 capture, such as activated carbons,[7] zeolites,[8] silicas,[9] MOFs, and COFs.[10] MOFs have maintained a position at the forefront of such studies, owed to their highly crystalline nature, tunable structures, and record porosity.[11-13] Unfortunately, many MOFs suffer from issues, such as low CO_2 capacity and selectivity, particularly in the presence of humidity,[14-15] and short lifetime. Thus, to enhance their performance, numerous efforts have been made to develop post-synthetic modification (PSM) strategies that can be used to decorate the inside of MOFs with basic groups, like amines. Such studies are predominately focused on impregnation approaches, where low molecular weight molecules or polymers are allowed to diffuse into the MOF pores.[16-18] In such studies, the amines are physically adsorbed on the internal framework wall and/or chemisorbed onto open metal coordination sites.[18-20] When such interactions are weak, they can lead to amine leaching, particularly in humid environments, limiting performance with extensive cycling.[21] For instance, Milner et al. reported the displacement of light weight amines from the metal surfaces in an amine functionalized MOF, Mg_2(dobpdc) (dobpdc = dihydroxy biphenyl dicarboxylic acid), in humid flue gas streams during temperature swing processes used for material regeneration.[21] This could be overcome by introducing tetraamines that were crosslinked between two Mg centers in the MOF.[22-23]

In an effort to prevent amine leaching, us and others have worked on the PSM of MOF ligands with pendant amines that are covalently grafted to the ligand backbone. While there are only a few articles reporting amine grafting to MOF ligands,[24-27] to date, such approaches have failed to significantly enhance the CO_2 uptake in the pressure regime of interest for post-combustion CO_2 capture. For example, in one previous report, PEI (polyethylene imine) was grafted onto an amine ligand in the UiO-66-NH_2 MOF. Albeit that there was an enhanced CO_2 adsorption at low pressures,[26] there was no experimental evidence of successful grafting and there was no cycling data in simulated flue gas streams. We also previously reported grafting amines to the NH_2-group on the NH_2-BDC (amino-terephthalic acid) ligand of Zn-BDC-NH_2 (also known as IRMOF-3) using bromoacetyl bromide as a bridging molecule.[27] Albeit the grafting could be quantified, the CO_2 adsorption capacity in the low pressure regime was minimally enhanced relative to the parent MOF (0.13 to 0.16 mmol/g at 0.15 bar and 313 K, respectively). Moreover, the material was highly moisture sensitive making its application in humid gas separations impossible. Thus, herein, we report the same PSM strategy carried out in a more robust MOF. In the present work, the MOF, known as NH_2-Cr-BDC, (alternatively known as NH_2-MIL-101-Cr) was modified with four different amines of varying length and size, including ethylenediamine (ED), diethylenetriamine (DETA), tris(2-aminoethyl)amine (TAEA) and Polyethylene imine (PEI, 800 MW). Next, the modified materials were assessed for post-combustion carbon capture. Notably, there is a positive correlation between the density of primary amines on the CO_2 capacity, selectivity, and binding energy. Interestingly, the amine composites also offered an improved CO_2 separation in a simulated flue gas mixture containing 15 % CO_2 and 85 % N_2 (~80 % RH). Further, the materials offer impressive performance over 200 continuous adsorption/desorption cycles. Last, after soaking the two best performing materials, TAEA and PEI grafted materials, in water, the CO_2 adsorption capacity remains the same with no signs of amine leaching. On the contrary, when the same MOF is impregnated with low molecular weight amines (TAEA) using traditional approaches, significant leaching is observed.

2. Results and discussion

2.1. Synthesis and Characterizations of amine composites

NH_2-Cr-BDC was synthesized via a reported protocol[28] (See Supplementary Information, Materials and Methods). The material is constructed from 2-aminoterephthalic acid (NH_2-BDC) and $Cr_3(\mu\text{-}O)$ core forming a MOF having the following chemical formula: $Cr_3O(X)(H_2O)_2(NH_2\text{-}BDC^{2-})_3$ (X = OH^-, NO_3^-). The as-synthesized NH_2-Cr-BDC MOF is crystalline and phase pure (Figure S1 a); the broad diffraction peaks come from the nano-size of the crystals, which have an average size of 34.0 ± 6.1 nm (Figure S1 c). The MOF was activated at 150 °C for 12 h under dynamic vacuum to access the surface area and pore volume. Nitrogen adsorption measurements, carried out at 77 K, reveal a BET surface area (S_{BET}) of ~2400 m^2/g and a pore volume of 1.6 cm^3/g (Figure S1 b). The MOF exhibits a three-dimensional porous structure with two different pore windows that are ~1.2 nm and 1.6 nm in diameter[28] and cages that are ~2.7 nm and 3.5 nm in diameter (Figure S1 b inset); these structural features can facilitate the diffusion of reagents in and out of the material.

For PSM-1, NH_2-Cr-BDC was mixed with 1, 2 or 3 equivalents of bromoacetyl bromide (BrAcBr) per $NH_2\text{-}BDC^{2-}$ ligand in THF, which was stirred for 60 min in an ice-bath and then 30 min at room temperature (RT). The concentration of BrAcBr was varied to maximize the appendage of BrAcBr onto the $NH_2\text{-}BDC^{2-}$ ligands. The obtained product, denoted as BrAc-NH-Cr-BDC, is still crystalline and pure as indicated by the PXRD pattern (Figure S2 a). The N_2 adsorption at 77 K showed a gradual drop in the S_{BET} from ~2400 m^2/g of the bare NH_2-Cr-BDC to 1785, 1620 and 1530 m^2/g, for 1 equiv., 2 equiv. and 3 equiv. of BrAcBr, respectively (Figure S2 b); this drop indicates incorporation of organics in the pore. The proof of functionalization was further confirmed using Fourier-transform infrared spectroscopy (FTIR). A band representative of a carbonyl (-C=O) stretching vibration of the amide appears at 1705 cm^{-1} after PSM-1 (Figure 1 a). In addition to this, the two stretching vibrations associated with primary amines ($-NH_2$) at 3388 cm^{-1} and 3500 cm^{-1} present in the bare MOF decreased in intensity after PSM-1, and a new band, which is representative of the stretching vibration of secondary amines (-NH-) appears at 3300 cm^{-1} (Figure 1 a); this confirms the successful transformation of the $NH_2\text{-}BDC^{2-}$ ligand to BrAc-NH-BDC^{2-}.Unfortunately, despite being treated with an excess of BrAcBr (3 equiv.) the stretching vibration of the primary amine on NH_2-Cr-BDC remains, implying that there is less than 100 % ligand conversion. Further insight into the nature of the functionalization was provided by the Br 3d region of XPS data.[29] NH_2-Cr-BDC treated with 3 equiv. of BrAcBr showed intense peaks at binding energies (BE) of 70.37 and 71.42 eV ($3d_{5/2}$ and $3d_{3/2}$, respectively), which are assigned to C-Br interactions (Figure 1 c, blue) and indicative of successful grafting. Interestingly, additional peaks were also observed at lower BE of 68.16 and 69.2 and eV ($3d_{5/2}$ and $3d_{3/2}$, respectively), which are assigned to inorganic Br species ($NH_3^+Br^-$ and Cr-Br) (Figure 1 c, red). However, because the BE of these proposed inorganic Br species are similar, [30-31] it is difficult to distinguish them via XPS analysis. While the complexity associated with the different possible inorganic species makes fully understanding the chemistry and quantifying the speciation after PSM-1 challenging. The XPS data could be fit to quantify the amount of organic and inorganic Br; the results indicate that there is a contribution from ~ 54 % organic species (C-Br contributions) and a 46 % inorganic Br species (Cr-Br, $NH_3^+Br^-$) (See Table S1). Since XPS is a surface sensitive technique, and the MOF crystal size is ~ 34 nm, XPS results were expected to resemble bulk characterization techniques. Despite this, the ligand modification in PSM-1 was also quantified from X-ray Absorption Spectroscopy (XAS), which provides more information on the bulk sample (see Supplementary information).

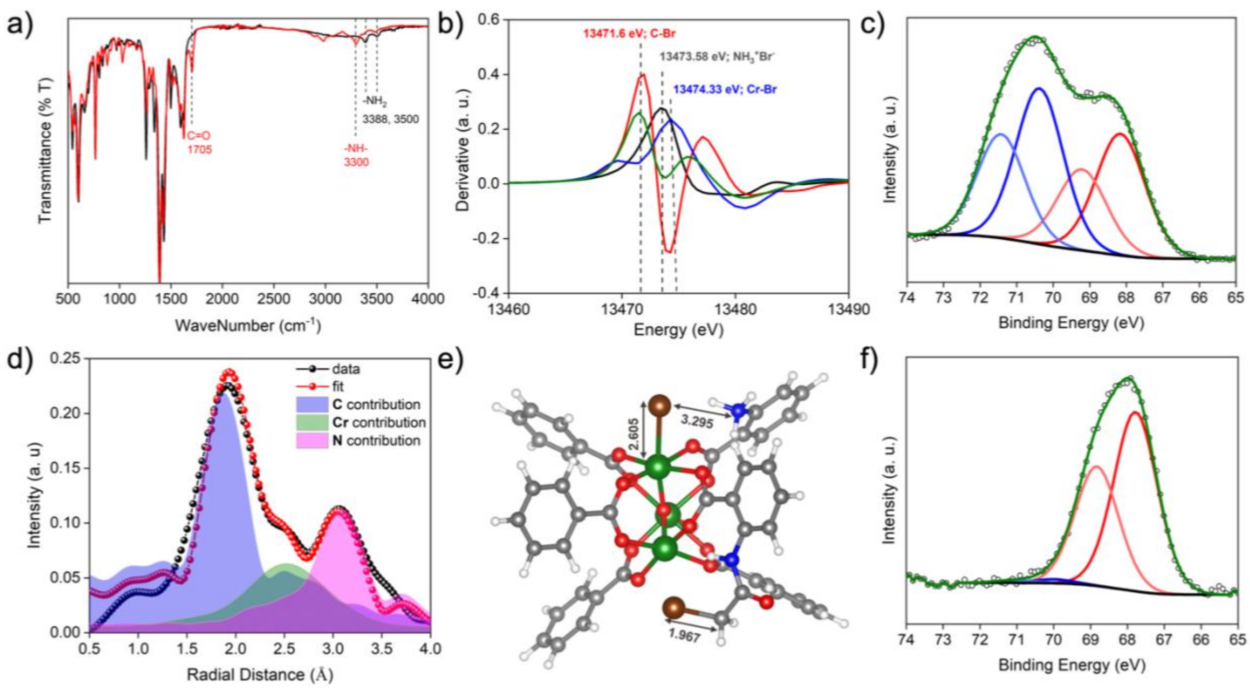

Figure 1: a) Infrared spectrum of NH_2-Cr-BDC (black), and 3 equiv. BrAcBr (red) reacted NH_2-Cr-BDC; b) XANES of Br K-edge of Br-Ac-NH-Cr-BDC (olive) is compared with reference samples $CH_3NH_3^+Br^-$ (black), BrAc-NH-BDC (red) and $CrBr_3$ (blue), d) EXAFS data obtained for BrAc-NH-Cr-BDC (black) and the fit (red) and e) Simulated cluster of NH_2-Cr-BDC with BrAcBr reaction on the ligand, XPS of Br 3d region for c) BrAc-NH-Cr-BDC and f) TAEA-Ac-NH-Cr-BDC; organic Br (blue) and inorganic Br (red), data (black hollow sphere), fit (olive).

The XAS data collected for the NH_2-Cr-BDC treated with 3 equiv. of BrAcBr was fit using three reference samples, including the modified BrAc-NH-BDC ligand (referred to as organic Br, C-Br), $CrBr_3$ (referred to as inorganic Br, Cr-Br) and $CH_3NH_3^+Br^-$ (also referred to as inorganic Br as $NH_3^+Br^-$). The first derivative of X-ray Absorption Near Edge Spectroscopy (XANES) of the references was compared to BrAc-NH-Cr-BDC. The absorption energy of PSM-1 at 13,471.6 eV matches with the C-Br of the reference sample BrAc-NH-BDC, indicating a major contribution from C-Br, which stems directly from the ligand grafting (Figure 1 b). In addition, there is a shoulder at 13,476 eV, which lies in the same area as that of the reference samples, $CH_3NH_3^+Br^-$ (13,473.58 eV) and $CrBr_3$ (13,474.33 eV), indicating the existence of inorganic Br^- including $NH_3^+Br^-$ and CrBr (Figure 1 b). The quantity of each Br species could be determined after a linear fitting of the three reference samples. The data indicates that there is 46 % organic Br (C-Br bonds), 31.6 % Cr-Br, and 22.4 % $NH_3^+Br^-$; these values are close to those obtained from XPS analysis (Figure S3). It is noted that, for every ligand modification with BrAcBr in NH_2-Cr-BDC, one H^+ and Br^- is released, which then has an opportunity to protonate unreacted NH_2-BDC ligands and/or the anion could bind to the Cr^{3+} cluster via exchange with OH^-/NO_3^-. Knowing this, EXAFS (Extended X-ray Absorption Fine Structure) data was then collected on BrAc-NH-Cr-BDC to extract structural information on the atoms in close proximity to Br (Figure 1 d). To further explore the complexes formed during the functionalization of the MOF with BrAcBr, Kohn-Sham density functional methods (DFT) were employed. For this, the MOF system was reduced to representative cluster models of the pristine material with the OH^- counter ion exchanged by Br^- (Figure S4) and the MOF upon PSM-1 (Figure 1e). The methods used in the complementary computational study are well described in the SI. In Figure 1e, the framework after PSM-1 is modeled by a cluster containing -NH-AcBr and -NH_2 functionalization on two benzoates as well as H^+ and Br^- that are released during the modification.[32] It was found in the simulations that the Br^- ion is in close proximity to the Cr^{3+} site, which is also adjacent to the unreacted, but protonated NH_2-BDC ligand; this indicates that the Br^- could have a dual electrostatic interaction with both Cr^{3+} and NH_3^+ (Figure 1 e). The optimized atom distances of the simulated cluster model (Figure 1 e) are then compared to the radial distances obtained from with the EXAFS spectrum. The peaks found at 1.93 Å, 2.54 Å, and 3. 1 Å in the EXAFS data are in close correlation to C-Br distance (1.967 Å), Cr^{3+}-Br (2.605 Å) and the NH_3^+-Br (3.295 Å) distances (Figure 1 d-e) obtained from DFT. The DFT calculation also suggests that the interaction between Br^- and NH_3^+ on the adjacent ligand, weaken the Cr-Br interaction. This can be observed by a slight elongation of the Cr-Br bond in the PSM-1 cluster when compared to the Cr-Br distance of 2.48 Å found in the cluster model of the pristine MOF (Figure S4).

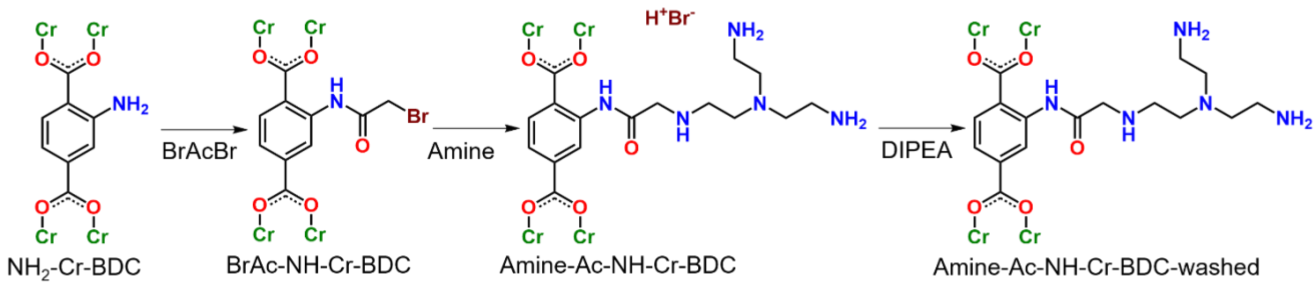

Scheme 1: PSM strategy of amine grafting to the ligand of MOF NH_2-Cr-BDC. The scheme shows PSM-1 with BrAcBr, PSM-2 with the appendage of an alkyl amine, and a base washing step to deprotonate the amine**.**

With 46% of the NH_2-Cr-BDC ligands functionalized with BrAcBr, PSM-2 was subsequently carried out. This process consisted of a reaction between BrAc-NH-Cr-BDC and 3 equivalents of various alkylamines (Scheme 1). The reaction employed ED, DETA, TAEA, or PEI in THF for 60 min at 1-4 ^oC and then 30 min at RT. The successful conversion of BrAc-NH-Cr-BDC to Amine-Ac-NH-Cr-BDC was then probed by Br 3d region of XPS data. For this, one of the amine-grafted composites, TAEA-Ac-NH-Cr-BDC was used, which showed only a very minor contribution of ~2 % of C-Br and ~98 % of inorganic Br (Cr-Br/$NH_3^+Br^-$) (Figure 1 f, Table S1). This indicates that there is ~98 % conversion of the BrAc-functionalized ligands to the amine functionalized ones, gives a total conversion of ~45 % of NH_2-BDC ligand functionalized with amines. All four resulting products obtained after PSM-2 were found to be crystalline and phase pure as indicated by PXRD (Figure S5 a). Next, the materials were subsequently activated at 120 ^oC for 12 h under vacuum to access the S_{BET} and pore volume after amine functionalization. The N_2 adsorption at 77 K revealed S_{BET} ranging from ~320 to 1570 m^2/g after amine grafting, implying that the materials are still highly porous (Figure S6 and Table S2). It is noted that the drop in surface area correlates with the quantity and size of the added amine; for instance, the S_{BET} drop was higher for the bulkiest amine, PEI, while it was lower for TAEA (0.46 nm radii) and the linear amines, DETA (0.8 nm length) and ED (0.54 nm length). TGA also revealed higher organic content for the composite produced from PEI (~56 wt %) grafting than for TAEA, DETA, and ED (Figure S7, Table S2). Notably, the Amine-Ac-NH-Cr-BDC samples had 6-7 wt % quantities of Br^- still in the pores as indicated by Ion Chromatography (IC); so, it was hypothesized that the samples still contained a large quantity of protonated amines (Table S3).[27] Owed to our desire to employ the materials in post-combustion carbon capture, the amine appended samples were washed with N,N-Diisopropylethylamine (DIPEA) in MeOH for 30 minutes. This process was meant to deprotonate residual amine-based salts in the structure as such species have a lower affinity towards CO_2 relative to their deprotonated counterparts.[27] The washed products, denoted as Amine-Ac-NH-Cr-BDC-washed, were found to be crystalline and phase pure (Figure S5 b). Importantly, a significant decrease in the Br^- content to less than 2 wt % was observed for all composites via IC after the DIPEA wash (Table S3). The elemental analysis also showed a slight increase in N and C content due to the removal of Br^- (Table S3). This is further supported by TGA data, which reveals a decrease in the residual weight % for all composites, for example from 36.9 wt % to 34.6 wt %, after burning off organics in TAEA-Ac-NH-Cr-BDC after washing. This decrease in residual mass implies that the net organic content with Br contribution is reduced after the wash (Figure S7 b and Table S2). The decrease in organic content is further supported by N_2 adsorption data collected at 77 K; the S_{BET} slightly increased for DETA and TAEA functionalized MOF by ~100 m^2/g (Figure S6, Table S2) after the DIPEA washing. However, no significant change in surface area was observed for the ED and PEI functionalized MOF.

2.2. CO_2 adsorption studies

After PSM-2, used to graft amines inside the MOF pores, the CO_2 adsorption performance of each material was studied. For this, the amine-functionalized MOFs, both before and after the DIPEA wash, were activated at 120 °C for 12 h under dynamic vacuum. Next, CO_2 adsorption was measured at 313 K, a temperature of interest for post-combustion carbon capture. Among the small chain polyamines ED, DETA and TAEA, the best-performing material was TAEA-Ac-NH-Cr-BDC, which has a CO_2 uptake of 0.8 mmol CO_2/g at 313 K and 0.15 bar (Figure S8) and is further increased to 1 mmol CO_2/g with the DIPEA wash (Figure 2 a). The CO_2 uptake was enhanced for all amine composites upon Br^- removal by the DIPEA wash (Figure 2 a, Figure S8). This stems from the fact that the base wash transforms the amine salts (like $NH_3^+Br^-$) into the deprotonated form (R-NH_2), which has a higher affinity for CO_2. For comparison, the CO_2 uptake at 313 K and 0.15 bar is 0.48, 0.7, and 1.0 mmol/g for ED-Ac, DETA-Ac- and TAEA-Ac-NH-Cr-BDC-washed, respectively. Further, the better performance of TAEA-Ac-NH-Cr-BDC-washed is related to the higher density of primary amines when compared to ED and DETA. Given this, it was hypothesized that other polyamines having more primary amines would further boost capacity. To test this, PEI having a molecular weight of 800 g/mol was also grafted onto the MOF ligand forming PEI-Ac-NH-Cr-BDC. Albeit that PXRD indicates that the PEI grafted composite is crystalline, the low angle peaks are suppressed likely due to pore filling, which is a common behavior observed for PEI incorporated porous frameworks, MIL-101(Cr)[16] (Figure S5). Despite this, as hypothesized, the CO_2 uptake was enhanced to 1.18 and 1.55 mmol/g at 0.15 bar and 313 K for the PEI-Ac-NH-Cr-BDC and

PEI-Ac-NH-Cr-BDC-washed, respectively; this is nearly 35% higher than the TAEA-Ac-NH-Cr-BDC-washed composite (Figure 2 a and Figure S8).

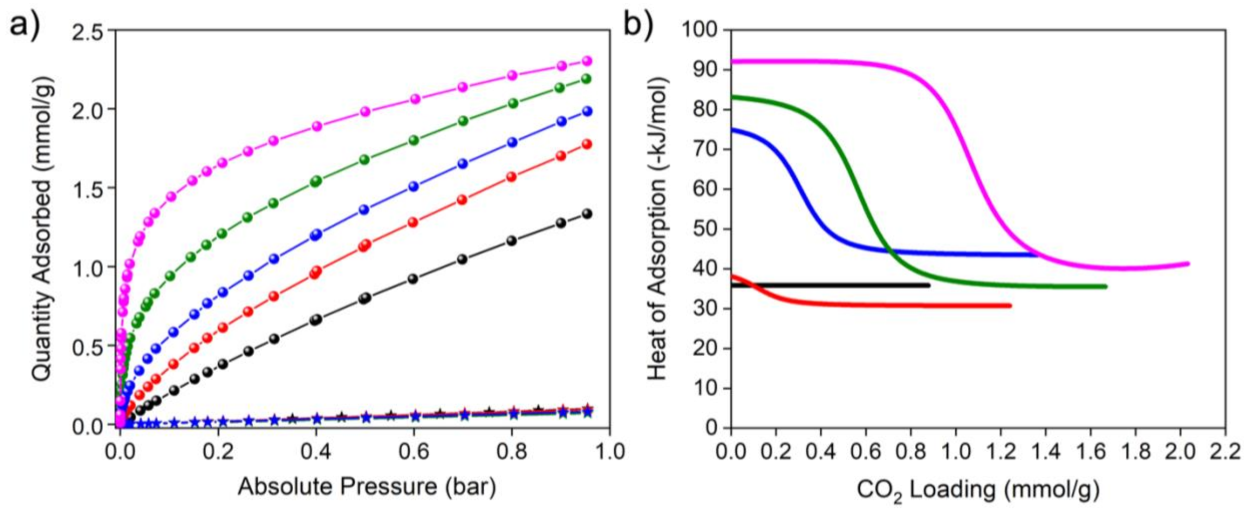

Figure 2: a) CO_2 and N_2 isotherms at 313 K for amine-Ac-NH-Cr-BDC-washed composites; CO_2 (spheres), N_2 (stars) b) Q_{st} of CO_2 adsorption of amine-Ac-NH-Cr-BDC after DIPEA wash; NH_2-Cr-BDC (black), ED-Ac-NH-Cr-BDC-washed (red), DETA-Ac-NH-Cr-BDC-washed (blue), TAEA-Ac-NH-Cr-BDC-washed (olive) and PEI-Ac-NH-Cr-BDC-washed (magenta).

To further assess the performance of the material for post-combustion carbon capture, other thermodynamic parameters like CO_2/N_2 (15/85) selectivity and isosteric heats of CO_2 adsorption (Q_{st}) were determined for all materials. For the parent MOF, NH_2-Cr-BDC, the CO_2/N_2 selectivity at 313 K was found to be 18.7 via the IAST model (See Supplementary information). As expected, modification with the amines significantly increased the CO_2/N_2 selectivity to, 26.5, 74.7 and 265 for DETA-Ac-, TAEA-Ac- and PEI-Ac-NH-Cr-BDC before washing, respectively (Figure S8). Notably, no enhancement in selectivity was observed for ED-Ac-NH-Cr-BDC. After amine deprotonation, the selectivity was further boosted to 32.8, 57.0 98.75 and 437 for ED-Ac-, DETA-Ac-, TAEA-Ac- and PEI-Ac-NH-Cr-BDC-washed, respectively (Figure 2 a), due to the higher CO_2 affinity. The isosteric heat of CO_2 adsorption was subsequently calculated using variable temperature adsorption isotherms (298 K, 313 K and 333 K). The isotherms were subsequently fit with Langmuir models and the isosteric heats of CO_2 adsorption were extracted using the Clausius-Clapeyron equation (See Supplementary information). Notably, a single site Langmuir model was used for the bare MOF, NH_2-Cr-BDC and ED-Ac-NH-Cr-BDC, while a dual site Langmuir model was used for the rest of the amine composites (Figure S9-S12, Table S4-S7). As expected, the Q_{st} lies in the physisorption regime for the parent NH_2-Cr-BDC MOF, -

36 kJ/mol, and ED-Ac-NH-Cr-BDC-washed, -38 kJ/mol (Figure 2 b). The latter is in correlation with the literature reports for porous organic frameworks decorated with ED.[33] On the contrary, grafting molecules that contain a larger number of amines to the internal pore surface increases the Q_{st} significantly to -75 kJ/mol, -83 kJ/mol and -92 kJ/mol for DETA-Ac-, TAEA-Ac- and PEI-Ac-NH-Cr-BDC-washed composites, respectively (Figure 2 b). This stems from the formation of a higher density of chemisorbed species like carbamates, and stabilization of these chemisorbed species by hydrogen bonds from the adjacent amines (-NH-).[27, 33] It was shown previously that each additional H-bond interaction with a chemisorbed CO_2 can add additional 17 kJ/mol.[33] Such H-bond interactions are absent in the ED-Ac-functionalized material due to the lack of free, adjacent -NH- groups. As expected, the Q_{st} for the protonated, unwashed analogs are significantly lower with values of -33 kJ/mol, -66 kJ/mol, -78.6 kJ/mol and -86 kJ/mol for ED-Ac-DETA-Ac-, TAEA-Ac- and PEI-Ac-NH-Cr-BDC, respectively (Figure S13). This of course stems from the presence of salt species, like $NH_3^+Br^-$, which have a lower affinity for CO_2.[27] For instance, a previous study showed that the charged salt species, $NH_3^+Br^-$, form a CO_2 adduct ($CO_2^{\delta-}$) via the interaction between Br^- and CO_2, as well as H-bonding interactions between the H of $NH_3^+Br^-$ and the O of the $CO_2^{\delta-}$ adduct.[27] Such interactions are weaker than those that occur for carbamate species, where there is a direct nucleophilic attack from the lone pair of electrons of an amine on the C of the CO_2.

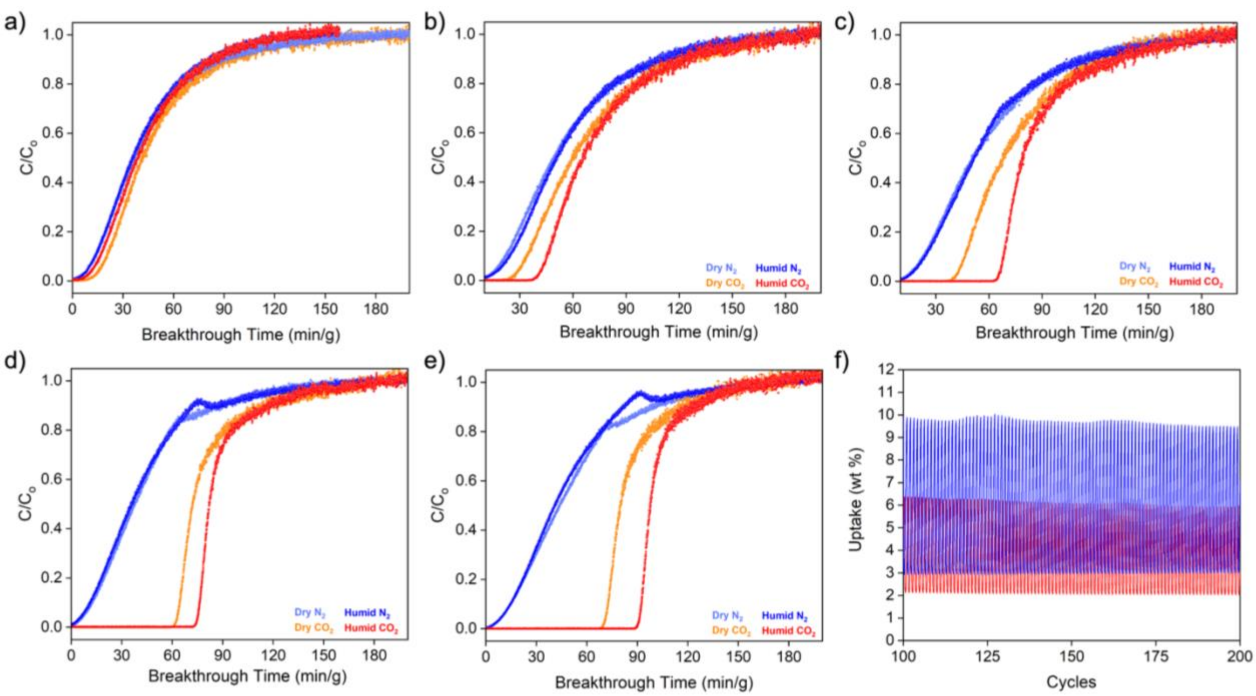

Figure 3: CO_2/N_2 breakthrough separation data collected at 313 K in a mixture containing 15 % CO_2 and 85 % N_2 mixture. The material was tested in both dry and at ~80 % RH; dry N_2 (light blue), humid N_2

(dark blue), dry CO_2 (orange) and humid CO_2 (red); a) NH_2-Cr-BDC, and then the MOF functionalized with b) ED-Ac-, c) DETA-Ac-, d) TAEA-Ac-, e) PEI-Ac-NH-Cr-BDC-washed and f) Last 100 TSA cycles of TAEA-Ac- (red) and PEI-Ac-NH-Cr-BDC-washed (blue) at 40 ^oC adsorption in 15 % CO_2, 85 % N_2 and 80 % RH for 7 min and desorption at 100 ^oC in 100 % CO_2 at 80% RH for 7 min.

Next, the kinetic performance of the amine-Ac-NH-Cr-BDC-washed samples were assessed in a simulated post-combustion flue gas stream containing 15 % CO_2 and 85 % N_2 under dry and humid conditions (80 % relative humidity, RH). For this, breakthrough (BT) studies were conducted at 313 K by flowing the simulated flue gas mixture through a column of length 10.5 cm containing ~0.2 g of the activated MOF composite and ~0.2 g of glass beads. For the humid tests, the bed was pre-saturated with 80 % RH for 2 h using a He flow rate of 2 mL/min, prior to passing a humid CO_2/N_2 (15/85) gas mixture through the adsorbent column. For the parent MOF, the breakthrough separation time was 10 min/g in a dry CO_2/N_2 mixture and 3 min/g in the humid stream (Figure 3 a). This decline is likely due to competitive adsorption of water molecules over CO_2 at the available adsorption sites. On the contrary, ED-Ac-, DETA-Ac-, TAEA-Ac- and PEI-Ac-NH-Cr-BDC-washed had much improved breakthrough separation times of 15, 25, 61, and 70 min/g, respectively, in dry conditions (Figure 3). In humid conditions there is an even greater enhancement as the breakthrough times increase to 25, 52, 74, and 90 min/g for ED-Ac- to DETA-Ac- to TAEA-Ac- to PEI-Ac-NH-Cr-BDC-washed, respectively (Figure 3 a-e and Table 1). It is noted that these values are 8, 17, 25 and 30 times larger than the original parent MOF, NH_2-Cr-BDC, that was also tested in the wet flue gas stream (Figure 3). The effective CO_2 capacity was also calculated from breakthrough data (Figure S14, Table S8, see SI for details). The best performing materials, TAEA-Ac- and PEI-Ac-NH-Cr-BDC-washed, have capacities of ~1.05 mmol/g and 1.23 mmol/g, respectively, in humid conditions (Table S8). Whereas in dry conditions, the capacity is found to be slightly lower, 0.87 and 0.97 mmol/g for TAEA-Ac- and PEI-Ac-NH-Cr-BDC-washed, respectively. On the contrary, the bare MOF shows CO_2 capacities of 0.24 mmol/g in dry mixture, which decreased to 0.097 mmol/g in humid gas mixtures. The reason for such observation is that, for the amine composites, in wet streams there is the formation of bicarbonates/carbamic acid, which involves an amine to CO_2 ratio of 1:1, whereas in dry conditions, the CO_2 absorption occurs via carbamate formation, which involves an amine to CO_2 ratio of 2:1 (Figure S15).[34] Thus, in wet conditions, the CO_2 capacity is boosted. Last, the trend observed during the CO_2/N_2 kinetic separation (ED-Ac- < DETA-Ac- < TAEA-Ac- < PEI-Ac-NH-Cr-BDC-washed) correlates well with the trends observed for thermodynamic parameters including low-pressure CO_2 capacity, CO_2 affinity, and CO_2/N_2 selectivity.

Table 1: Summary of CO_2 adsorption properties at amine-Ac-NH-Cr-BDC-washed composites at 313 K.

Composite	CO_2 at 0.15 bar (mmol/g)	CO_2/N_2 (15/85) selectivity	Q_{st} (-kJ/mol)	Breakthrough separation time dry (min/g)	Breakthrough separation time humid (min/g)
NH_2-Cr-BDC	0.28	18.7	36	10	3
ED-Ac-NH-Cr-BDC-washed	0.48	32.8	38	15	25
DETA-Ac-NH-Cr-BDC-washed	0.7	57	75	25	52
TAEA-Ac-NH-Cr-BDC-washed	1.0	98.75	83	61	74
PEI-Ac-NH-Cr-BDC-washed	1.55	437	92	70	90

Next, the cyclability of the best performing materials were tested in a simulated flue gas stream. For this, TAEA-Ac- and PEI-Ac-NH-Cr-BDC-washed were subjected to 200 rapid TSA cycles. Adsorption was carried out in ~15 % CO_2 and 85 % N_2 (80 % RH) at 40 ^{o}C, while desorption was done at 100 ^{o}C in highly humid CO_2 (with 7-minute adsorption and desorption cycles). Given that both water and CO_2 adsorb at 40 ^{o}C, the humid CO_2 uptake is presented in terms of overall wt %. Notably, after the first few cycles (~up to 10), the adsorption has a nearly 2-3 weight % loss for both samples (Figure S16-17 a); this could stem from two scenarios. First, strongly adsorbed CO_2 or H_2O may not be released at the desorption temperature of 100 ^{o}C. Second, there could also be rapid amine degradation, for instance, via the irreversible formation of urea species. Notably, previous reports show that humidity can inhibit such amine degradation, and instead promote the formation of carbamate/bicarbonate species.[34] Notable, while FTIR measurements provide no conclusive indication of amine degradation (urea or amide formation), $-NH_2^+$ and -NH-deformations are observed in the range 1570-1615 cm^{-1}[35] after cycling. The latter likely indicates that not all of the chemisorbed CO_2 on the primary amines (carbamates, $NH_2^+CO_2^-$) is fully desorbed at 100

°C. Hence, limited desorption is likely the culprit for a large portion of this initial drop. Albeit that the data also shows a slight shift in the -C=O stretching vibration of the amine-Ac-NH-Cr-BDC after cycling from 1684 cm^{-1} to 1669-1674 cm^{-1} (Figure S18), we are unable to state with certainty whether this results from additional H-bonding interactions between adsorbed water and -C=O or the formation of linear urea species [36]. Notably, after cycle 25, the base line in the TGA plot stabilizes for both materials (Figure S16-17 b), indicating that there is minimal amine leaching (as would be indicated by a dropping baseline) or degradation into urea species with cycling (as would be indicated by a rising baseline). In fact, the cyclable capacities are found to be 4 wt % for TAEA and 6.6 wt % for PEI composites after 200 cycles (Figure 3 f). Despite the absence of significant amine loss and urea formation after 25 cycles, we do still note a slight decrease in the overall quantity of adsorbed species for both samples. We hypothesized that this could stem from three phenomena. First, the CO_2 concentration could gradually decrease over time due to dilution by the counter gas stream (pure N_2) or absorption in the water bubbler. Second, there could be a slow degradation of the MOF during the rapid TSA cycles blocking amine access. Third, the amines could gradually transform into other species, like imine and nitrile, owed to oxygen impurities present during the TGA experiment.[37] Notably, the PXRD patterns of the samples after cycling do not indicate MOF degradation (Figure S19). In an effort to eliminate the possibility of CO_2 dilution, the cycling experiment of TAEA-Ac-NH-Cr-BDC-washed was stopped and restarted after cycle 200 and then continued to cycle 270. While we note that the material's adsorption capacity recovers to some degree, it is an incomplete recovery (Figure S20). Unfortunately, from the FTIR data, it is not possible to determine if the amines transform into imine or nitrile species. Thus, at this stage, we believe that CO_2 dilution and amine transformation could both play a role in the dropping performance after cycle 25. Hence, more extensive cycling studies under varying desorption conditions are required in the future for us to better understand the mechanism behind the performance decline.

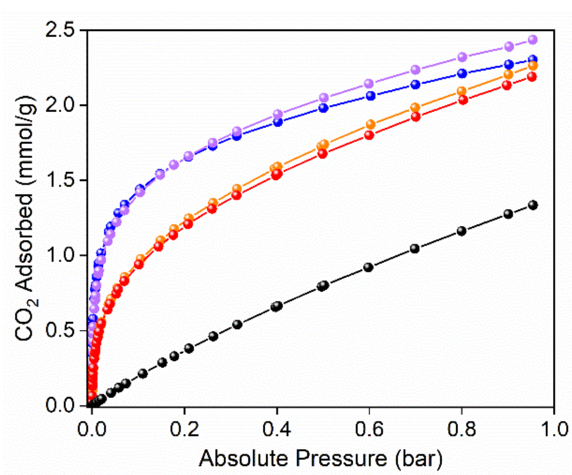

Figure 4: CO_2 adsorption isotherms at 313 K of bare MOF (black), as-synthesized TAEA-Ac-NH-Cr-BDC-washed (red), water-soaked TAEA-Ac-NH-Cr-BDC-washed (orange) as-synthesized PEI-Ac-NH-Cr-BDC-washed (blue) and water soaked PEI-Ac-NH-Cr-BDC-washed (violet); Soaked in water for 1 h.

Last, to prove that the amines are truly grafted to the MOF ligand and they do not leach out, the best performing materials, including TAEA-Ac- and PEI-Ac-NH-Cr-BDC-washed were soaked in water for 1 h at RT, and subsequently vacuum dried. As expected, the framework remained intact (Figure S21), and the CO_2 adsorption isotherms measured at 313 K show no loss of CO_2 capacity when compared to the as-synthesized amine grafted material (Figure 4). For comparison, the NH_2-Cr-BDC MOF was also impregnated with TAEA and PEI using traditional approaches that employ cyclohexane as a solvent;[17] afterwards, the impregnated samples were subjected to the same soaking treatment. In this case, there is a significant decline in CO_2 performance for both materials. For instance, the CO_2 adsorption capacity of TAEA impregnated NH_2-Cr-BDC was 2.5 mmol/g at 0.15 bar and 313 K; however, after soaking in water for 1 h, the CO_2 adsorption capacity drops to just 0.4 mmol/g, which is an ~85 % decline (Figure S22 a). For PEI, due to the high viscosity and insolubility of PEI in cyclohexane, the material became more like a slurry (Figure S22 b inset image). Thus, the initial CO_2 adsorption isotherms could not be measured due to amine leaching during the measurements. However, the obtained slurry was subjected to the same treatment in water for 1 h. The CO_2 adsorption at 313 K and 0.15 bar was found to be 1.1 mmol/g, which is already 30% lower than that of PEI grafted composite, PEI-Ac-NH-Cr-BDC-washed, 1.55 mmol/g (Figure S22 b). Thus, this study highlights that impregnated amines can readily leach from MOF pores, while covalently grafting the amines can inhibit leaching, and hence enhance the lifetime of the material.

3. Conclusions

The work presented here demonstrates a two-step strategy used to covalently graft amines inside the pores of a robust MOF known as NH_2-Cr-BDC, for post-combustion carbon capture applications. In this work, bromoacetyl bromide (BrAcBr) is used as a bridge between the amine-decorated MOF ligand and several alkyl amines including ethylenediamine (ED), diethylenetriamine (DETA), tris(2-aminoethyl) amine (TAEA), and low-molecular weight polyethyleneimine (PEI). Various performance metrics, including CO_2 uptake, CO_2/N_2 selectivity, and isosteric heats of CO_2 adsorption (Q_{st}), were obtained for the parent MOF and each amine-appended counterpart. Notably, all amine-decorated materials offered a significant improvement in CO_2 adsorption performance relative to the parent MOF. Moreover, as the number of primary amines and overall amine density is increased, the CO_2 performance could be readily enhanced. The best performer in all tests was the sample denoted as PEI-Ac-NH-Cr-BDC-washed, which had the highest density of primary amines. The material offered 1.55 mmol/g CO_2 uptake at 313 K and 0.15 bar, an IAST CO_2/N_2 selectivity of 437, and a Q_{st} of -92 kJ/mol. Also, the breakthrough time was improved by a factor of 30 relative to the parent MOF when tested under humid conditions and a high cyclable capacity of 6.6 wt % was achieved even after 200 TSA cycles. Finally, by covalently grafting amines to the ligand, there is no change in the CO_2 adsorption isotherms for materials before and after soaking; however, when compared to the same material simply impregnated with amines using traditional approaches, there is a significant loss in the CO_2 adsorption capacity, up to ~85%, after soaking. It is hoped that amine grafting strategies like this one, can offer future benefits in terms of adsorbent lifetime, when compared to adsorbents where amines are simply physiosorbed in the pores of the porous support.

4. Materials and method

All chemicals were obtained from commercial sources and used as received without further purification. Chromium nitrate nonahydrate, $Cr(NO_3)_3.9H_2O$ (Acros, 98 %), 2-aminoterephthalic acid, NH_2-BDC (ABCR, 98 %), bromoacetyl bromide, BrAcBr (ABCR, 98 %), tetrahydrofuran, THF (Roth, 99.5 %), N,N-dimethylformamide, DMF (Roth, 99.5 %), Acetonitrile, ACN (Roth, 99.5 %) ethylenediamine, ED (TCI, 98 %) diethylenetriamine, DETA (TCI, 98 %), tris(2-aminoethyl)amine, TAEA (ABCR, 98 %), Polyethyleneimine, PEI (800 MW) (Sigma Aldrich, 99 %), N,N-Diisopropylethylamine, DIPEA (ABCR, 98 %).

Synthesis of NH_2-Cr-BDC: A 160 mL Teflon autoclave was charged with 6.4 g of $Cr(NO_3)_3.9H_2O$, 2.898 g of 2-amino-terephthalic acid (NH_2-BDC^{2-}), 1.28 g of sodium hydroxide, and 120 mL DI water. The mixture was first stirred for 15 min and sonicated for 15 min prior to transferring to a 160 mL autoclave. The oven was heated to 150 ^oC for 1 h at 150 ^oC for 12 h and cooled to 25 ^oC in 4 h. Once the reaction was finished, the bright green product was separated into four 50 mL centrifuge tubes and washed with 40 mL water once, 40 mL DMF three times, and 40 mL EtOH three times and then refluxed with 200 mL EtOH at 90 ^oC for 12 h two times. The resulting product was vacuum dried at RT overnight and further vacuum dried at 80 ^oC for 6 h. The sample was activated at 150 ^oC for 12 h under dynamic vacuum to access the surface area and CO_2 adsorption properties.

Synthesis of Bromoacetyl functionalized MOF (PSM-1): For the first step of PSM, 440 mg of as-synthesized NH_2-MIL101(Cr) was dispersed in 20 mL THF. The temperature was adjusted to 1-4 ^oC with an ice bath. Then, different equivalents of bromoacetyl bromide, BrAcBr (1 equiv., 140 µL 2equiv., 280 µL and 3 equiv., 420 µL) with respect to the NH_2-BDC ligand was added to the cold solution and allowed to stir for 1h in the ice bath and then at RT for an additional 30 min. After the reaction, the product was centrifuged and washed with 40 mL fresh THF two times and vacuum dried for spectroscopic characterization.

Synthesis of amine grafted composite (Amine-Ac-NH-Cr-BDC) PSM-2: For the second step of PSM with amines, the prepared samples after PSM-1 (without drying) was dispersed in 40 mL THF at 1-4 ^oC. Then, three equivalents of ED (0.328 mL), DETA (0.5 mL), TAEA (0.72 mL) or PEI (2.8 mL) (with respect to the NH_2-BDC^{2-}) were added to the cold solution and allowed to react for 1 h in the ice bath and then 30 additional min at RT under stirring. After the reaction, the product was washed with 80 mL MeOH and vacuum dried. The sample was activated at 120 ^oC under dynamic vacuum before assessing the porosity and CO_2 adsorption at different temperatures.

Synthesis of amine grafted composite washed (Amine-Ac-NH-Cr-BDC-washed): The product obtained from PSM-2, approximately ~480 mg (without drying) was dispersed in 40 mL MeOH and 4 mL DIPEA. The sample was shaken vigorously in a vortex machine for 30 min to deprotonate the amines and remove the excess Br^- from the framework. The product was washed with 80 mL MeOH and vacuum dried. The sample was activated at 120 ^oC under dynamic vacuum before assessing the porosity and CO_2 adsorption at different temperatures.

Synthesis of amine impregnated NH_2-Cr-BDC: 100 mg of activated NH_2-Cr-BDC is added to a mixture of 8 mL cyclohexane and 0.18 mL TAEA or 0.2 mL PEI respectively and stirred for 5 min. The composites are centrifuged and washed with excess cyclohexane and vacuum dried at RT. The samples were activated at 120 ^oC under dynamic vacuum to access the CO_2 adsorption performance at 313 K.

Synthesis of water soaked composites: About 100 mg of TAEA-Ac- and PEI-Ac-NH-Cr-BDC-washed are soaked in 10 mL water in a 15 mL centrifuge tube and shaken in a vortex shaker for 1 h. The composites are then centrifuged and washed with water one time and MeOH one time and vacuum dried at RT for 1 day. The sample were activated at 120 ^oC under dynamic vacuum before assessing the CO_2 adsorption at 313K.

Supporting Information

The description of the characterization tools, calculation methods, Powder X-ray diffraction, TEM, XAS and XPS fitting, CO_2 and N_2 adsorption isotherms and fitting, Gas breakthrough (BT) data, CO_2 breakthrough capacity calculations, Temperature Swing Adsorption/Desorption (TSA) cycles, FTIR and TGA are included in the Supplementary information.

Acknowledgement

This work was supported by the Swiss National Science Foundation under grant numbers 200021_188536 and PYAPP2_160581. We thank GAZNAT for the support of J. E. We thank Dr. Natalia Gasilova for her help with Microwave digestion of samples and Dr. Olga Trukhina for the help with IC measurements.

References

[1]. Masson-Delmotte, V., P. Zhai, H.-O. Pörtner, D. Roberts, J. Skea, P.R. Shukla, A. Pirani, W. Moufouma-Okia, C. Péan, R. Pidcock, S. Connors, J.B.R. Matthews, Y. Chen, X. Zhou, M.I. Gomis, E. Lonnoy, T. Maycock, M. Tignor, and T. Waterfield (eds.) *IPCC 2018: Global Warming of 1.5°C.An IPCC Special Report on the impacts of global warming of 1.5°C above pre-industrial levels and related global greenhouse gas emission pathways, in the context of strengthening the global response to the threat of climate change, sustainable development, and efforts to eradicate poverty*.

[2]. IPCC, 2014: Climate Change 2014: Synthesis Report. Contribution of Working Groups I, II and III to the Fifth Assessment Report of the

Intergovernmental Panel on Climate Change [Core Writing Team, R.K. Pachauri and L.A. Meyer (eds.)]. IPCC, Geneva, Switzerland, 151 pp. **2014**.

[3]. Metz, B., O. Davidson, H. C. de Coninck, M. Loos, and L. A. Meyer (eds.), IPCC, 2005: IPCC Special Report on Carbon Dioxide Capture and Storage. Prepared by

Working Group III of the Intergovernmental Panel on Climate Change. . *Cambridge University*

Press, Cambridge, United Kingdom and New York, NY, USA, 442 pp. **2005**.

[4]. Rochelle Gary, T., Amine Scrubbing for CO2 Capture. *Science* **2009,** *325* (5948), 1652-1654.

[5]. Sumida, K.; Rogow, D. L.; Mason, J. A.; McDonald, T. M.; Bloch, E. D.; Herm, Z. R.; Bae, T.-H.; Long, J. R., Carbon Dioxide Capture in Metal–Organic Frameworks. *Chemical Reviews* **2012,** *112* (2), 724-781.

[6]. Weiland, R. H.; Dingman, J. C.; Cronin, D. B., Heat Capacity of Aqueous Monoethanolamine, Diethanolamine, N-Methyldiethanolamine, and N-Methyldiethanolamine-Based Blends with Carbon Dioxide. *Journal of Chemical & Engineering Data* **1997,** *42* (5), 1004-1006.

[7]. Faisal, M.; Pamungkas, A. Z.; Krisnandi, Y. K., Study of Amine Functionalized Mesoporous Carbon as CO2 Storage Materials. *Processes* **2021,** *9* (3).

[8]. Chatterjee, S.; Jeevanandham, S.; Mukherjee, M.; Vo, D.-V. N.; Mishra, V., Significance of re-engineered zeolites in climate mitigation – A review for carbon capture and separation. *Journal of Environmental Chemical Engineering* **2021,** *9* (5), 105957.

[9]. Bollini, P.; Didas, S. A.; Jones, C. W., Amine-oxide hybrid materials for acid gas separations. *Journal of Materials Chemistry* **2011,** *21* (39), 15100-15120.

[10]. Zeng, Y.; Zou, R.; Zhao, Y., Covalent Organic Frameworks for CO2 Capture. *Advanced Materials* **2016,** *28* (15), 2855-2873.

[11]. Lin, J.-B.; Nguyen Tai, T. T.; Vaidhyanathan, R.; Burner, J.; Taylor Jared, M.; Durekova, H.; Akhtar, F.; Mah Roger, K.; Ghaffari-Nik, O.; Marx, S.; Fylstra, N.; Iremonger Simon, S.; Dawson Karl, W.; Sarkar, P.; Hovington, P.; Rajendran, A.; Woo Tom, K.; Shimizu George, K. H., A scalable metal-organic framework as a durable physisorbent for carbon dioxide capture. *Science* **2021,** *374* (6574), 1464-1469.

[12]. Furukawa, H.; Cordova Kyle, E.; O'Keeffe, M.; Yaghi Omar, M., The Chemistry and Applications of Metal-Organic Frameworks. *Science* **2013,** *341* (6149), 1230444.

[13]. Guillerm, V.; Kim, D.; Eubank, J. F.; Luebke, R.; Liu, X.; Adil, K.; Lah, M. S.; Eddaoudi, M., A supermolecular building approach for the design and construction of metal–organic frameworks. *Chemical Society Reviews* **2014,** *43* (16), 6141-6172.

[14]. Erucar, I.; Keskin, S., Unlocking the Effect of H2O on CO2 Separation Performance of Promising MOFs Using Atomically Detailed Simulations. *Industrial & Engineering Chemistry Research* **2020,** *59* (7), 3141-3152.

[15]. Kizzie, A. C.; Wong-Foy, A. G.; Matzger, A. J., Effect of Humidity on the Performance of Microporous Coordination Polymers as Adsorbents for CO2 Capture. *Langmuir* **2011,** *27* (10), 6368-6373.

[16]. Lin, Y.; Yan, Q.; Kong, C.; Chen, L., Polyethyleneimine Incorporated Metal-Organic Frameworks Adsorbent for Highly Selective CO2 Capture. *Scientific Reports* **2013,** *3* (1), 1859.

[17]. Li, H.; Wang, K.; Hu, Z.; Chen, Y.-P.; Verdegaal, W.; Zhao, D.; Zhou, H.-C., Harnessing solvent effects to integrate alkylamine into metal–organic frameworks for exceptionally high CO2 uptake. *Journal of Materials Chemistry A* **2019,** *7* (13), 7867-7874.

[18]. Choe, J. H.; Kim, H.; Hong, C. S., MOF-74 type variants for CO2 capture. *Materials Chemistry Frontiers* **2021,** *5* (14), 5172-5185.

[19]. Siegelman, R. L.; McDonald, T. M.; Gonzalez, M. I.; Martell, J. D.; Milner, P. J.; Mason, J. A.; Berger, A. H.; Bhown, A. S.; Long, J. R., Controlling Cooperative CO2 Adsorption in Diamine-Appended Mg2(dobpdc) Metal–Organic Frameworks. *Journal of the American Chemical Society* **2017,** *139* (30), 10526-10538.

[20]. McDonald, T. M.; Lee, W. R.; Mason, J. A.; Wiers, B. M.; Hong, C. S.; Long, J. R., Capture of Carbon Dioxide from Air and Flue Gas in the Alkylamine-Appended Metal–Organic Framework mmen-Mg2(dobpdc). *Journal of the American Chemical Society* **2012,** *134* (16), 7056-7065.

[21]. Milner, P. J.; Martell, J. D.; Siegelman, R. L.; Gygi, D.; Weston, S. C.; Long, J. R., Overcoming double-step CO2 adsorption and minimizing water co-adsorption in bulky diamine-appended variants of Mg2(dobpdc). *Chemical Science* **2018,** *9* (1), 160-174.

[22]. Peh Shing, B.; Zhao, D., Tying amines down for stable CO2 capture. *Science* **2020,** *369* (6502), 372-373.

[23]. Kim Eugene, J.; Siegelman Rebecca, L.; Jiang Henry, Z. H.; Forse Alexander, C.; Lee, J.-H.; Martell Jeffrey, D.; Milner Phillip, J.; Falkowski Joseph, M.; Neaton Jeffrey, B.; Reimer Jeffrey, A.; Weston Simon, C.; Long Jeffrey, R., Cooperative carbon capture and steam regeneration with tetraamine-appended metal–organic frameworks. *Science* **2020,** *369* (6502), 392-396.

[24]. Britt, D.; Lee, C.; Uribe-Romo, F. J.; Furukawa, H.; Yaghi, O. M., Ring-Opening Reactions within Porous Metal−Organic Frameworks. *Inorganic Chemistry* **2010,** *49* (14), 6387-6389.

[25]. Molavi, H.; Joukani, F. A.; Shojaei, A., Ethylenediamine Grafting to Functionalized NH2–UiO-66 Using Green Aza-Michael Addition Reaction to Improve CO2/CH4 Adsorption Selectivity. *Industrial & Engineering Chemistry Research* **2018,** *57* (20), 7030-7039.

[26]. Zhu, J.; Wu, L.; Bu, Z.; Jie, S.; Li, B.-G., Polyethyleneimine-Modified UiO-66-NH2(Zr) Metal–Organic Frameworks: Preparation and Enhanced CO2 Selective Adsorption. *ACS Omega* **2019,** *4* (2), 3188-3197.

[27]. Justin, A.; Espín, J.; Kochetygov, I.; Asgari, M.; Trukhina, O.; Queen, W. L., A Two Step Postsynthetic Modification Strategy: Appending Short Chain Polyamines to Zn-NH2-BDC MOF for Enhanced CO2 Adsorption. *Inorganic Chemistry* **2021,** *60* (16), 11720-11729.

[28]. Jiang, D.; Keenan, L. L.; Burrows, A. D.; Edler, K. J., Synthesis and post-synthetic modification of MIL-101(Cr)-NH2via a tandem diazotisation process. *Chemical Communications* **2012,** *48* (99), 12053-12055.

[29]. Smykalla, L.; Shukrynau, P.; Korb, M.; Lang, H.; Hietschold, M., Surface-confined 2D polymerization of a brominated copper-tetraphenylporphyrin on Au(111). *Nanoscale* **2015,** *7* (9), 4234-4241.

[30]. Wu, Y.; Zhu, M.; Zhao, R.; Liu, X.; Shen, J.; Huang, H.; Shen, S.; Zhang, L.; Zhang, J.; Zheng, X.; Wang, S., Degradation Effect and Magnetoelectric Transport Properties in CrBr3 Devices. *Materials* **2022,** *15* (9).

[31]. Liao, M.; Yu, B.-B.; Jin, Z.; Chen, W.; Zhu, Y.; Zhang, X.; Yao, W.; Duan, T.; Djerdj, I.; He, Z., Efficient and Stable FASnI3 Perovskite Solar Cells with Effective Interface Modulation by Low-Dimensional Perovskite Layer. *ChemSusChem* **2019,** *12* (22), 5007-5014.

[32]. M. J. Frisch, G. W. T., H. B. Schlegel, et al., *Gaussian˜16 Revision C.01,*

Gaussian Inc. Wallingford CT **2016**.

[33]. Thirion, D.; Rozyyev, V.; Park, J.; Byun, J.; Jung, Y.; Atilhan, M.; Yavuz, C. T., Observation of the wrapping mechanism in amine carbon dioxide molecular interactions on heterogeneous sorbents. *Physical Chemistry Chemical Physics* **2016,** *18* (21), 14177-14181.

[34]. Sayari, A.; Belmabkhout, Y., Stabilization of Amine-Containing CO2 Adsorbents: Dramatic Effect of Water Vapor. *Journal of the American Chemical Society* **2010,** *132* (18), 6312-6314.

[35]. Heacock, R. A.; Marion, L., THE INFRARED SPECTRA OF SECONDARY AMINES AND THEIR SALTS. *Canadian Journal of Chemistry* **1956,** *34* (12), 1782-1795.

[36]. Choi, W.; Min, K.; Kim, C.; Ko, Y. S.; Jeon, J. W.; Seo, H.; Park, Y.-K.; Choi, M., Epoxide-functionalization of polyethyleneimine for synthesis of stable carbon dioxide adsorbent in temperature swing adsorption. Nature Communications 2016, 7 (1), 12640.

[37]. Utsumi, T.; Noda, K.; Kawauchi, D.; Ueda, H.; Tokuyama, H., Nitrile Synthesis by Aerobic Oxidation of Primary Amines and in situ Generated Imines from Aldehydes and Ammonium Salt with Grubbs Catalyst. Advanced Synthesis & Catalysis 2020, 362 (17), 3583-3588